NANO LETTERS

LETTER

pubs.acs.org/NanoLett

Time-Domain ab Initio Study of Auger and Phonon-Assisted Auger Processes in a Semiconductor Quantum Dot

Kim Hyeon-Deuk*,† and Oleg V. Prezhdo*,‡

†Department of Chemistry, Kyoto University, Kyoto, 606-8502, Japan

‡Department of Chemistry, University of Rochester, Rochester, New York 14642, United States

ABSTRACT: We developed time-domain ab initio simulation of Auger phenomena, including multiple exciton generation (MEG) and recombination (MER). It is the first approach describing phonon-assisted processes and early dynamics. MEG starts below the electronic threshold, strongly accelerating with energy. Ligands are particularly important to phonon-assisted MEG, which therefore can be probed with infrared spectroscopy. Short-time Gaussian component gives 5−10% of MEG, justifying rate theories that assume exponential dynamics. MER is preceded by electron−phonon relaxation to low energies.

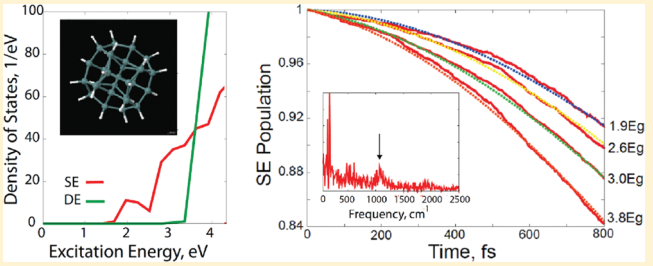

KEYWORDS: Quantum dot, Auger processes, multiple-exciton generation, electron−phonon interactions, time-domain density functional theory, nonadiabatic molecular dynamics

Auger processes constitute an essential component of excited state evolution in most nanoscale materials. Confinement of charge carriers enhances charge scattering by reducing the average distance between particles and increasing Coulomb interactions. Auger processes govern exciton[1−4] and charge[5] dynamics in semiconductor quantum dots (QDs) and affect QD blinking.[6] They influence optical absorption[7] and photoluminescence[8] of carbon nanotubes, charge carriers in graphene,[9] and electron−hole plasma in metallic nanowires.[10] Even loosely bound van der Waals clusters exhibit efficient Auger scattering.[11] Auger spectroscopy provides a powerful tool for investigating structure,[12] evolution,[13] spin-polarization,[14] and chemistry[15] of surface species. It can be used to monitor electronic processes in molecular, nanoscale, and biological systems with attosecond time resolution.[16]

Auger dynamics in semiconductor QDs are particularly important for photovoltaics. Photons absorbed at the blue end of the solar spectrum create high-energy excitations that relax to the lowest energy harvested in the red. Significant amounts of solar power are lost to heat, limiting photovoltaic efficiency to 31%.[17] Multiple exciton recombination (MER) by the Auger mechanism can further accelerate energy losses by transferring photon energy to the charge carrier that is more strongly coupled to phonons.[18] On the contrary, the inverse process, known as impact ionization,[17,19] uses the excess energy to excite additional electrons across the band gap, resulting in carrier multiplication[1] and multiple exciton generation[2] (MEG). MEG can raise the photovoltaic efficiency to 44%.[1−4,17]

Despite the large body of work devoted to MEG in QDs and other nanoscale materials, drastically different opinions exist regarding its mechanism and efficiency.[1−4,19−26] Most theoretical studies allow systematic investigation of MEG as a function of QD size, energy, and semiconductor type.[19,25−28] At the same time, they usually apply to weak perturbative Coulomb coupling, assume exponential decay, and describe one process at a time. A comprehensive picture should include simultaneously forward and inverse Auger dynamics, phonon-assisted Auger processes, and electron−phonon relaxation and dephasing. Additionally, one would like to model the effect of QD ligands, dopants, charges, defects, etc. The desired description is provided by time-domain ab initio simulation[29] that most closely mimics the experimental studies.[1−10,16,30,31] Such simulation can give a novel and comprehensive perspective on the scattering dynamics of excited charge carriers in nanoscale materials that are key to solar energy harvesting, plasmonics, electronics, spintronics, surface chemistry, etc.[1−16,32]

This Letter reports the first time-domain atomistic simulation of Auger dynamics in a nanoscale system. The approach combines ab initio time-domain density functional theory (TDDFT) with nonadiabatic molecular dynamics (NAMD), which have been tested many times with dozens of systems. However, this is the first application of TDDFT-NAMD to Auger processes. Compared to other theories, our approach is nonperturbative and correctly treats short-time dynamics. Further, it incorporates not only elastic Auger scattering but also inelastic processes, including phonon-assisted Auger events and electron−phonon relaxation. Since Auger phenomena dominate excitation dynamics in most nanoscale materials, the developed technique should find multiple applications extending far beyond this first study. Focusing on a semiconductor QD, we study MEG and MER dynamics and find that MEG accelerates with energy, in agreement with other theories. For the first time, we establish

Received: February 25, 2011
Revised: March 20, 2011
Published: March 31, 2011

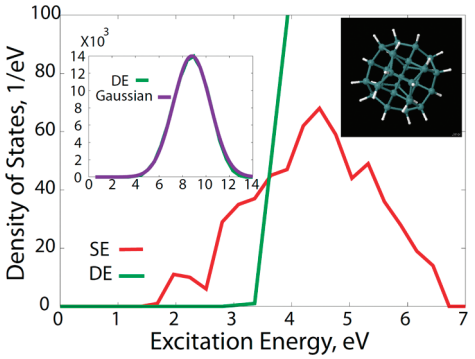

Figure 1. SE and DE densities in $Ge_{29}H_{24}$. There are 600 SE and 97500 DE states in the simulation. Above a threshold, DEs are much denser than SEs, and can be well fitted by the Gaussian, $24500\ \exp[-(x-8.8)^2]/5$. The $Ge_{29}H_{24}$ structure is shown in the top-right corner.

clearly that MEG can be assisted by phonons at energies below the electronic threshold. High-frequency ligand modes are particularly important for phonon-assisted MEG, suggesting that the latter can be probed experimentally with infrared spectroscopy. At energies above the threshold only intrinsic QD phonons contribute to MEG. In this case, acoustic modes are more important than optical modes, as determined by selection rules for electron−phonon coupling. The short-time Gaussian dynamics show much weaker energy dependence than the long-term exponential processes. We determine that the Gaussian component contributes under 10% to overall MEG, justifying rate theory models that assume exponential decay. We find that electron−phonon relaxation competes successfully with MER. MER becomes efficient only at low energies, after a significant amount of energy has been deposited into phonon modes by the relaxation.

Photon absorption initiates complex electron−phonon dynamics in semiconductor QDs. One or several electrons can be promoted from the valence band (VB) to the conduction band (CB), depending on optical selection rules and electron−hole interaction strength. High-energy electron−hole pairs, known as excitons, lose energy to heat by coupling to phonons. The lowest energy exciton lives for a long time, since nonradiative relaxation to the ground state is prevented by a substantial mismatch between the fundamental electronic energy gap, E_g, and the phonon frequencies. The ground state is recovered by fluorescence, and the emitted photon energy can be significantly lower than the energy of the absorbed photon. Surface defects due to unsaturated dangling bonds and missing atoms, as well as electronic states localized on the ligands, can generate charges and charged excitons by electron transfer between the QD core and the surface. This process is responsible for QD fluorescence blinking, since charge separated states do not emit light. Electrons and holes can exchange energy, accelerating the electron−phonon relaxation in materials such as CdSe, in which the VB is denser than the CB and holes relax faster than electrons. Alternatively, electron−hole scattering can generate additional excitons or destroy some of existing electron−hole pairs. These Auger processes and their competition with the electron−phonon relaxation constitute the focus of the current work.

The study focuses on a Ge QD, Figure 1. Ge belongs to the same group of the periodic table as Si, which is the most common solar cell material. Compared to Si, bulk Ge has a significantly lower band gap: 1.1 vs 0.67 eV, respectively. While MEG has

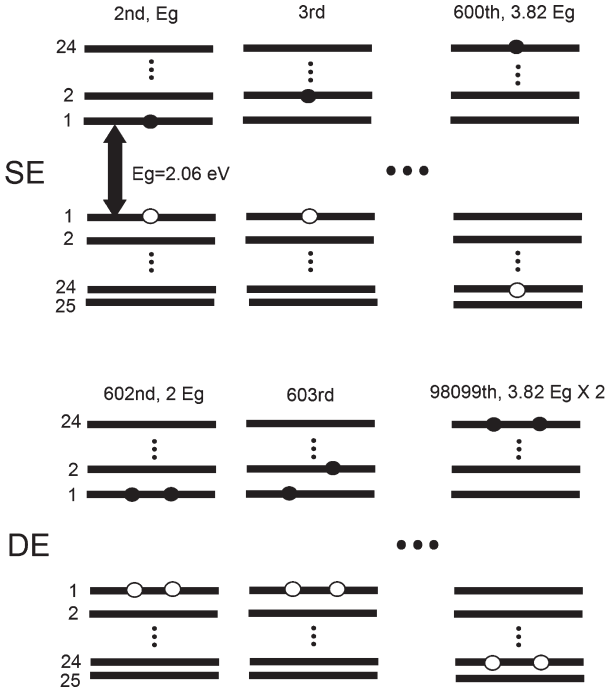

Figure 2. The SE and DE state basis. The calculated zero temperature energy gap is E_g = 2.06 eV. The first state is the ground state.

been observed in Si QDs,[33] the absolute excitation energies required for efficient MEG are rather high. Due to its lower band gap, Ge is a promising alternative to Si.[27,34] Although there exist no experimental data on MEG in Ge QDs yet, significant synthetic efforts are underway,[35,36] and one can expect that MEG will be investigated in Ge nanocrysals experimentally in the near future. The experimental data[1−4,28,33] and analytical models[26,27,37−41] find many common features for MEG in PbSe, CdSe, Si, and other materials. Thus, the conclusions obtained in our study of the Ge QD should hold qualitatively with other semiconductors QDs.

The electronic structure and adiabatic molecular dynamics were computed with VASP[42] using a converged plane-wave basis, PW91 functional, and projector-augmented-wave pseudopotentials. The bare Ge QD was passivated with hydrogen atoms shown in Figure 1 by white spheres. At room temperature, a 5 ps microcanonical trajectory was produced in the ground electronic state. The QD always preserved the bulk topology, and neither bond breaking nor other major changes in the QD atomic or electronic structure were observed during the simulation, leading to converged results.

The Auger dynamics involving single exciton (SE) and double exciton (DE) states coupled to atomic motions were simulated using TDDFT formulated in the adiabatic Kohn−Sham (KS) basis.[43−46] The evolution of the single-electron KS orbitals $\phi_p(\mathbf{r}, t)$ was determined using the standard equations[43]

$$i\hbar\frac{\partial\phi_p(\mathbf{r},t)}{\partial t} = H(\phi(\mathbf{r},t))\phi_p(\mathbf{r},t) \qquad (1)$$

$$p = 1, \ldots, N_e$$

where N_e is the number of electrons. The equations are coupled, since the Hamiltonian H depends on the density obtained by summing over all KS orbitals occupied by the N_e electrons.

dx.doi.org/10.1021/nl200651p |Nano Lett. 2011, 11, 1845–1850

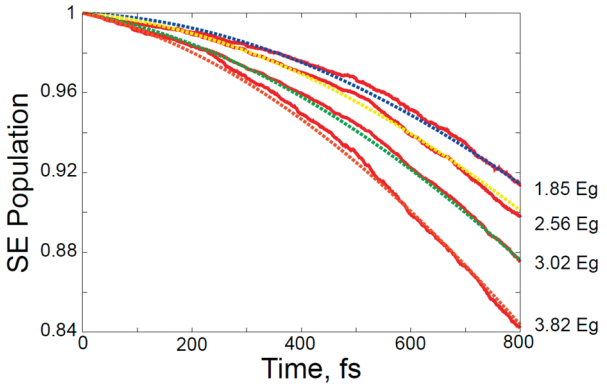

Figure 3. Decay of the combined population of all SEs due to ME generation, starting from the initially excited 158th ($1.85E_g$), 314th ($2.56E_g$), 418th ($3.02E_g$), and 600th ($3.82E_g$) SEs. The ground state population remains negligible within the shown time scale. The DE generation accelerates with increasing excitation energy. The data are fitted by $0.75\exp[-t^2/\tau_g{}^2] + 0.25\exp[-t/\tau_e]$ with τ_g/τ_e equal to 2.45/20.0, 2.39/10.0, 2.32/5.00, and 2.00/4.00 ps, from lowest to highest energy, respectively.

Expanding the time-dependent KS orbitals $\phi_p(\mathbf{r}, t)$ in the adiabatic KS orbital basis $\tilde{\phi}_k(\mathbf{r}; \mathbf{R})$

$$\phi_p(\mathbf{r}, t) = \sum_{k=1}^{N_e} c_{pk}(t)|\tilde{\phi}_k(\mathbf{r}; \mathbf{R})\rangle \tag{2}$$

transforms eq 1 into the equations for the expansion coefficients

$$i\hbar\frac{\partial c_{pk}(t)}{\partial t} = \sum_{m=1}^{N_e} c_{pm}(t)(\epsilon_m\delta_{km} - i\hbar\mathbf{d}_{km}\cdot\dot{\mathbf{R}}) \tag{3}$$

The adiabatic KS orbitals $\tilde{\phi}_k(\mathbf{r}; \mathbf{R})$ were obtained with DFT for current atomic positions along the trajectory. The NA coupling includes electron−phonon interaction

$$\mathbf{d}_{km}\cdot\dot{\mathbf{R}} = \langle\tilde{\phi}_k(\mathbf{r}; \mathbf{R})|\nabla_{\mathbf{R}}|\tilde{\phi}_m(\mathbf{r}; \mathbf{R})\rangle\cdot\dot{\mathbf{R}} = \left\langle\tilde{\phi}_k(\mathbf{r}; \mathbf{R})\left|\frac{\partial}{\partial t}\right|\tilde{\phi}_m(\mathbf{r}; \mathbf{R})\right\rangle \tag{4}$$

arising from the dependence of the adiabatic KS orbitals on the phonon dynamics $\mathbf{R}(t)$.

Figure 2 shows how the SE and DE states are formed by electron−hole excitations from the ground state. The 24 CB and 25 VB orbitals used in our calculations give rise to 600 SE and 97500 DE states. The ground, SE, and DE states form the electronic basis used in our study; each state can transit to another state due to the NA coupling. The Hamiltonian matrix appearing in the TD Schrödinger equation is too large for direct numerical simulation; the total number of states is 98101, resulting in 98101^2 = 9,623,806,201 Hamiltonian matrix elements. However, we found that the Hamiltonian is sparse, since each NA transition involves only a single electron or hole.[43] This very important numerical feature of our scheme allowed us to use sparse matrix techniques.

Considering the density of states (DOS) for SEs and DEs in $Ge_{29}H_{24}$ at room temperature, Figure 1, we observe that starting around 3.5 eV, the DE DOS is much larger than the SE DOS, since the combinatorial number of DEs grows significantly faster with energy than the number of SEs. At higher energies, DEs completely dominate over SEs, as evidenced by the *y*-axis scales shown in the main part and insert of Figure 1. Therefore, one can expect that the excited state population will be shifted to DEs at high energies and SEs at low energies, provided SEs and DEs are coupled.

Figure 3 describes MEG. It shows the population of all SE states as a function of time for different excitation energies. The decay of SEs is accompanied by the corresponding growth of MEs, since the total population of SEs and MEs is conserved. The ground state population remains negligible for the duration of the simulation, in agreement with nanosecond QD fluorescence lifetimes. The data are fitted well by the universal function, $0.75\exp[-t^2/\tau_g{}^2] + 0.25\exp[-t^2/\tau_e]$ with the time scale parameters reported in the figure caption. The dynamics show both Gaussian and exponential components. The initial decay of a quantum state is always Gaussian.[47] The decay becomes exponential at longer times, after the quantum dynamics have explored the Hilbert space. This is a common feature of many experimental and theoretical results. At short times the initial state couples to few other states and the dynamics is Rabi-like. Note that the Gaussian and Rabi-like sinusoidal functions coincide at short times. At long times the dynamics involve a large ensemble of final states and become exponential, as described for instance by Fermi's golden rule. Our explicit time-domain theory is able to describe both relaxation regimes, while simple rate theories give only the long-time exponential component. The calculations show that the Gaussian component of the decay takes half a picosecond. After this time, the decay of the SE population becomes exponential. The exponential decay is represented in Figure 3 by the linear behavior, corresponding to the first-order term in the Taylor expansion of the exponential function. The transition from the Gaussian to the exponential decay occurs when the SE population drops to 0.92−0.96, indicating that the short-time Gaussian dynamics is responsible for 5−10% of the overall decay. Since the contribution of the Gaussian component is quite small, our atomistic time-domain simulation validates the rate theory models that are limited to exponential decay.

The MEG rate exhibits strong energy dependence[19,25−28] that arises primarily from the strong energy dependence of the density of DE states, as shown in Figure 1. The exponential component varies with energy much more than the Gaussian component, as can be seen in the time constants reported in the caption to Figure 3. This is because the high density of final DE states cannot be explored at the earliest times. The 4−10 ps exponential time constants obtained in our work fall within the range of other theoretical estimates obtained for CdSe, InAs, and Si QDs using Fermi's golden rule[26,37−39] and for a PbSe QD using a phenomenological theory.[40] Note that in contrast to other theories, our study includes the phonon-assisted Auger process, represented in Figure 3 by the slow 20 ps exponential decay.

Further details regarding phonon-assisted MEG are provided by the spectra shown in Figure 4. The data were obtained by computing Fourier transforms of the energy gaps between the SE and DE states with energies indicated in each panel. The SE states were selected to correspond to the first three cases of MEG shown in Figure 3. The upper right panel represents SE that is very close to $2E_g$. The data indicate that both acoustic and optical modes of the QD facilitate phonon-assisted MEG. For this small QD the mode frequencies are around 100 and 500 cm^{-1}, respectively. Additionally, the top two panels exhibit a peak around 1000 cm^{-1}. This frequency corresponds to Ge−H vibrations, with H-atoms providing a crude model of ligands that present on the surface of colloidal QDs.[48,49]

dx.doi.org/10.1021/nl200651p |*Nano Lett.* 2011, 11, 1845–1850

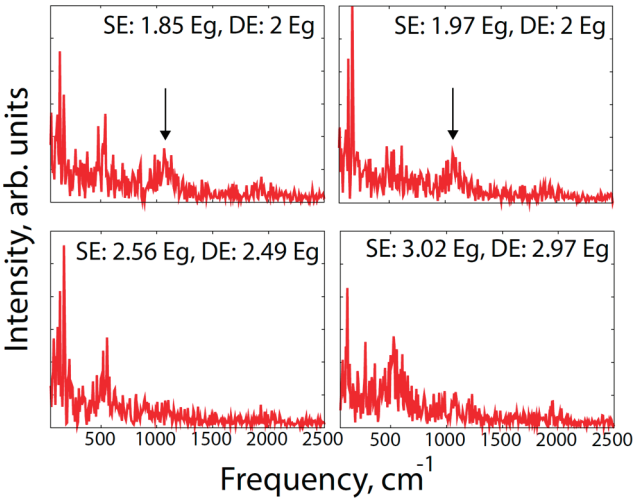

Figure 4. Phonon modes that participate in phonon-assisted MEG involving pairs of SE and DE states of slightly different energies. Both acoustic and optical modes of the QD at frequencies around 100 and 500 cm^{-1} facilitate the process. MEG starting from SEs below $2E_g$ is also assisted by phonon modes around 1000 cm^{-1} due to the Ge−H ligand bonds, top two panels. Comparison of phonon-assisted MEG at energies above $2E_g$ indicates that optical modes become more important at higher energies, bottom two panels.

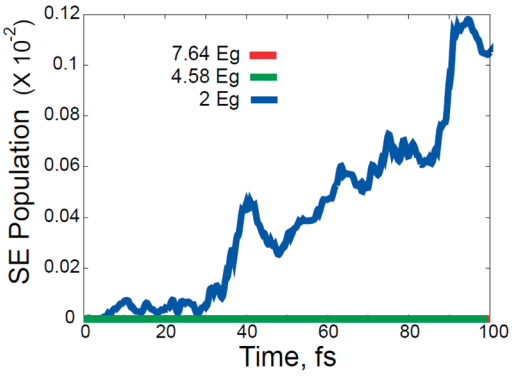

Figure 5. Generation of SEs due to ME recombination, starting from the initially excited 602nd ($2E_g$), 59291st ($4.58E_g$), and 98099th ($7.64E_g$) DEs. MER is preceded by electron−phonon relaxation, and only low energy DEs lead to SEs.

In general, the lower-frequency acoustic modes are more important than the higher frequency optical modes, Figure 4. This result for phonon-assisted Auger dynamics is consistent with our earlier simulations of electron−phonon relaxation.[29,45,46] Even though a priori one can expect that optical modes should be more important, due to the presence of the phonon velocity R in the NA coupling, the electronic part of the NA coupling in front of R creates a stronger selection rule, eq 4. At a given temperature, representing the average kinetic energy, R is higher for optical modes, which have smaller effective masses. However, the change in the electronic wave function caused by the phonon motion, given by $\nabla_R|\tilde{\phi}_m(\mathbf{r};\mathbf{R})>$, is more significant for acoustic modes. Acoustic modes alter the shape and size of the QD, thereby affecting the electronic wave functions that are delocalized over the whole dot. In contrast, optical modes generate local displacements of atoms with respect to each other. The effect of the local displacements tends to average out when integrated over the delocalized electronic wave functions.

The role of optical modes relative to acoustic modes grows with energy; compare the bottom two panels of Figure 4. A similar effect has been observed in our studies of carbon nanotubes.[44,50] Higher energy electronic states contain more nodes, and correspondingly, they are able to couple better to phonons that also have more nodes, i.e., optical phonons.

The upper two panels of Figure 4 show that ligands play a particularly important role for phonon-assisted MEG starting at energies below $2E_g$, as indicated by the peaks around 1000 cm^{-1}. The electronic degrees of freedom need to borrow energy from phonons, and the ligand mode provides the most energy per phonon. Experimentally, one can activate ligand modes by infrared spectroscopy. Therefore, it should be easily possible to study and control phonon-assisted MEG with lasers.

Next, consider MER. Figure 5 shows the population of SEs created starting from MEs of three different energies. The simulations clearly indicate that MER is much slower than MEG; compare the scales of the y axes in Figures 3 and 5. The simulations also show that MER is preceded by electron−phonon relaxation and occurs only from low energy DEs. A similar conclusion was obtained in the rate calculations.[27] Since the coupling between SEs and DEs promotes both forward and backward processes, the directionality is determined by the relative DOS for SEs and MEs, Figure 1. At high energies, SEs generate MEs, while at low energies MEs annihilate to form SEs.

Phonon-assisted Auger processes play an important role for MER; however, they cannot be detected as easily as in the case of MEG. Phonon-assisted MEG can be identified by MEG starting from SE states that are below the lowest energy ME at $2E_g$. The opposite is not true, since there are always SEs that are lower in energy than MEs. Phonon-assisted MER competes with electron−phonon relaxation that does not change the number of excitons. Our earlier study of the relaxation alone[45,46] shows that it is significantly faster than MER.

The current study is limited to a rather small QD, due to high computational cost of the calculations. As the dot size grows, the Coulomb coupling between SE and ME states will decrease. Consequently, the rates of the Auger processes drop as well.[37] The MEG threshold energy shows little dependence on cluster size, since it depends largely on the relative densities of the SE and ME states, which always cross slightly above $2E_g$.[27] The surface-to-volume ratio decreases with increasing cluster size. Therefore, the ligand contribution to the phonon-assisted Auger dynamics can be expected to decrease as well.

In summary, we have developed and performed for the first time ab initio simulations of MEG and MER dynamics in a semiconductor QD. Compared to other theories of Auger phenomena, our approach uniquely provides an atomistic time-domain description, directly mimics time-resolved experiments, properly treats early time evolution, and includes phonon-assisted Auger processes. The atomistic calculations reported here and the phenomenological, nonatomistic models[19,25−28,37−39] complement each other. The latter can be applied to QDs of any size. At the same time, they contain many adjustable parameters and are hard to generalize for studying atomistic details such as defects, ligands, dopants, etc. Although ab initio studies are limited to small clusters, they contain no adjustable parameters. Any parameter adjustment was done at a very basic level. Atomistic models can be applied to investigate defects, ligands, charges, dopants and dangling bonds, which play extremely important roles in the excitation dynamics of QDs.[24,29,45]

dx.doi.org/10.1021/nl200651p |Nano Lett. 2011, 11, 1845–1850

Since Auger processes dominate excitation and charge dynamics in most nanoscale systems, the developed approach can find many applications in the future.

Explicit time-domain simulations describe various dynamical regimes, including the short-time Gaussian and longer-time exponential components. The present simulations show that the Gaussian component of MEG contributes less than 10% to the overall process, thereby justifying those phenomenological models that are based on rate theories and assume exponential decay.[19,25−28,37−39] Our study indicates that both MEG and MER are strongly energy dependent; however, the energy dependence of MEG applies primarily to the long-time exponential dynamics. The initial Gaussian relaxation is much less sensitive to the initial energy. The MEG and MER rates depend on the initial and final state densities, which vary strongly with energy. While MEG accelerates with energy, MER decelerates. The simulations show that MER does not happen at all at high energies. It is preceded by electron−phonon relaxation and occurs at energies close to $2E_g$.

For the first time, we were able to study in detail phonon-assisted Auger phenomena and characterize the relevant phonon modes. We found that slow phonon-assisted MEG is possible from SEs slightly below $2E_g$. In this case, ligand modes become particularly important, since they provide the highest frequency phonons capable of donating significant amounts of energy to the electronic subsystem. At energies above $2E_g$ MEG is assisted by both optical and acoustic phonons of the QD. Acoustic phonons are generally more important than optical phonons due to the electron−phonon coupling selection rule. At higher energies the role of optical phonons increases due to a better match between their nodal structure and that of higher energy electronic states. The participation of ligand modes in phonon-assisted MEG suggests that the latter can be probed using infrared spectroscopy.

AUTHOR INFORMATION

Corresponding Author

*E-mail: kim@kuchem.kyoto-u.ac.jp, oleg.prezhdo@rochester.edu.

ACKNOWLEDGMENT

K.H.D. is partially supported by Grants-in-Aid for Scientific Research from the Japan Society for the Promotion of Science, Grant No. 20750010, and by the Global COE Program *Integrated Materials Science* (# B-09). O.V.P. acknowledges NSF Grant CHE-1050405 supporting the method development and DOE Grant DE-FG02-05ER15755 supporting the quantum dot studies.

REFERENCES

(1) Schaller, R. D.; Klimov, V. I. *Phys. Rev. Lett.* **2004**, *92*, 186601.
(2) Ellingson, R. J.; Beard, M. C.; Johnson, J. C.; Yu, P. R.; Micic, O. I.; Nozik, A. J.; Shabaev, A.; Efros, A. L. *Nano Lett.* **2005**, *5*, 865.
(3) Beard, M. C.; Midgett, A. G.; Hanna, M. C.; Luther, J. M.; Hughes, B. K.; Nozik, A. J. *Nano Lett.* **2010**, *10*, 3019.
(4) McGuire, J. A.; Sykora, M.; Joo, J.; Pietryga, J. M.; Klimov, V. I. *Nano Lett.* **2010**, *10*, 2049.
(5) Hendry, E.; Koeberg, M.; Wang, F; Zhang, H.; Donega, C. D.; Vanmaekelbergh, D.; Bonn, M. *Phys. Rev. Lett.* **2006**, *96*, 057408.
(6) Wang, X.; Ren, X.; Kahen, K.; Hahn, M. A.; Rajeswaran, M.; Maccagnano-Zacher, S.; Silcox, J.; Cragg, G. E.; Efros, A. L.; Krauss, T. D. *Nature* **2009**, *459*, 686.
(7) Huang, L. B.; Krauss, T. D. *Phys. Rev. Lett.* **2006**, *96*, 057407.
(8) Gabor, N. M.; Zhong, Z.; Bosnick, K.; Park, J.; McEuen, P. L. *Science* **2009**, *325*, 1367.
(9) George, P. A.; Strait, J.; Dawlaty, J.; Shivaraman, S.; Chandrashekhar, M.; Rana, F.; Spencer, M. G. *Nano Lett.* **2008**, *8*, 4248.
(10) Demichel, O.; Calvo, V.; Pauc, N.; Besson, A.; Noe, P.; Oehler, F.; Gentile, P.; Magnea, N. *Nano Lett.* **2009**, *9*, 2575.
(11) Averbukh, V.; Muller, I. B.; Cederbaum, L. S. *Phys. Rev. Lett.* **2004**, *93*, 263002.
(12) Trioni, M. I.; Caravati, S.; Brivio, G. P.; Floreano, L.; Bruno, F.; Morgante, A. *Phys. Rev. Lett.* **2004**, *93*, 206802.
(13) Ferralis, N.; Maboudian, R.; Carraro, C. *Phys. Rev. Lett.* **2008**, *101*, 156801.
(14) Unipan, M.; Robin, A.; Morgenstern, R.; Hoekstra, R. *Phys. Rev. Lett.* **2006**, *96*, 177601.
(15) Glass, S.; Nienhaus, H. *Phys. Rev. Lett.* **2004**, *93*, 168302.
(16) Ikeura-Sekiguchi, H.; Sekiguchi, T. *Phys. Rev. Lett.* **2007**, *99*, 228102.
(17) Nozik, A. J. *Annu. Rev. Phys. Chem.* **2001**, *52*, 193.
(18) Efros, A. L.; Kharchenko, V. A.; Rosen, M. *Solid State Commun.* **1995**, *93*, 281.
(19) Wang, L.-W.; Califano, M.; Zunger, A.; Franceschetti, A. *Phys. Rev. Lett.* **2003**, *91*, 056404.
(20) Beard, M. C.; Midgett, A. G.; Law, M.; Semonin, O. E.; Ellingson, R. J.; Nozik, A. J. *Nano Lett.* **2009**, *9*, 836.
(21) Nair, G.; Bawendi, M. G. *Phys. Rev. B* **2007**, *76*, 081304.
(22) Nair, G.; Geyer, S. M.; Chang, L.-Y.; Bawendi, M. G. *Phys. Rev. B* **2008**, *78*, 125325.
(23) Isborn, C. M.; Kilina, S. V.; Li, X.; Prezhdo, O. V. *J. Phys. Chem. C* **2008**, *112*, 18291.
(24) Fischer, S. A.; Isborn, C. M.; Prezhdo, O. V. *Chem. Sci.* **2011**, *2*, 400.
(25) Pijpers, J. J. H.; Ulbricht, R.; Tielrooij, K. J.; Osherov, A.; Golan, Y.; Delerue, C.; Allan, G.; Bonn, M. *Nat. Phys.* **2009**, *5*, 811.
(26) Rabani, E.; Baer, R. *Nano Lett.* **2008**, *8*, 4488.
(27) Luo, J. W.; Franceschetti, A.; Zunger, A. *Nano Lett.* **2008**, *8*, 3174.
(28) Schaller, R. D.; Agranovich, V. M.; Klimov, V. I. *Nat. Phys.* **2005**, *1*, 189.
(29) Prezhdo, O. V. *Acc. Chem. Res.* **2009**, *42*, 2005.
(30) Tisdale, W. A.; Williams, K. J.; Timp, B. A.; Norris, D. J.; Aydil, E. S.; Zhu, X. Y. *Science* **2010**, *328*, 1543.
(31) Sambur, J. B.; Novet, T.; Parkinson, B. A. *Science* **2010**, *330*, 63.
(32) Kempa, T. J.; Tian, B.; Kim, D. R.; Hu, J.; Zheng, X.; Lieber, C. M. *Nano Lett.* **2008**, *8*, 3456.
(33) Beard, M. C.; Knutsen, K. P.; Yu, P. R.; Luther, J. M.; Song, Q.; Metzger, W. K.; Ellingson, R. J.; Nozik, A. J. *Nano Lett.* **2007**, *7*, 2506.
(34) Chatterjee, S. *Sol. Energy* **2008**, *82*, 95.
(35) Lee, D. C.; Pietryga, J. M.; Robel, I.; Werder, D. J.; Schaller, R. D.; Klimov, V. I. *J. Am. Chem. Soc.* **2009**, *131*, 3436+.
(36) Ruddy, D. A.; Johnson, J. C.; Smith, E. R.; Neale, N. R. *ACS Nano* **2010**, *4*, 7459.
(37) Rabani, E.; Baer, R. *Chem. Phys. Lett.* **2010**, *496*, 227.
(38) Fu, Y.; Zhou, Y. H.; Su, H.; Boey, F. Y. C.; Agren, H. *J. Phys. Chem. C* **2010**, *114*, 3743.
(39) Califano, M. *Phys. Chem. Chem. Phys.* **2009**, *11*, 10180.
(40) Witzel, W. M.; Shabaev, A.; Hellberg, C. S.; Jacobs, V. L.; Efros, A. L. *Phys. Rev. Lett.* **2010**, *105*, 137401.
(41) Piryatinski, A.; Velizhanin, K. A. *J. Chem. Phys.* **2010**, *133*, 084508.
(42) Kresse, G.; Furthmuller, J. *Comput. Mater. Sci.* **1996**, *6*, 15.
(43) Craig, C. F.; Duncan, W. R.; Prezhdo, O. V. *Phys. Rev. Lett.* **2005**, *95*, 163001.
(44) Habenicht, B. F.; Craig, C. F.; Prezhdo, O. V. *Phys. Rev. Lett.* **2006**, *96*, 187401.
(45) Hyeon-Deuk, K.; Madrid, A. B.; Prezhdo, O. V. *Dalton Trans.* **2009**, *45*, 10069.
(46) Kilina, S. V.; Kilin, D. S.; Prezhdo, O. V. *ACS Nano* **2009**, *3*, 93.
(47) Prezhdo, O. V.; Rossky, P. J. *Phys. Rev. Lett.* **1998**, *81*, 5294.

(48) Dai, Y.; Cobley, C. M.; Zeng, J.; Sun, Y.; Xia, Y. *Nano Lett.* **2009**, *9*, 2455.
(49) Baker, J. L.; Widmer-Cooper, A.; Toney, M. F.; Geissler, P. L.; Alivisatos, A. P. *Nano Lett.* **2010**, *10*, 195.
(50) Habenicht, B. F.; Kamisaka, H.; Yamashita, K.; Prezhdo, O. V. *Nano Lett.* **2007**, *7*, 3260.